Supplementary Materials for:

Dynein achieves processive motion using both stochastic and coordinated stepping

Weihong Qiu[1,6], Nathan D. Derr[1,5,6], Brian S. Goodman[1], Elizabeth Villa[2,3], David Wu[3,4], William Shih[5], and Samara L. Reck-Peterson[1]

[1]Department of Cell Biology, Harvard Medical School, Boston Massachusetts, 02115, USA. [2]Department of Molecular Structural Biology, Max Planck Institute of Biochemistry, Martinsried, 82152, Germany. [3]Physiology Course, Marine Biological Laboratory, Woods Hole Massachusetts, 02543, USA. [4]Geffen School of Medicine, University of California, Los Angeles California, 90095, USA. [5]Dana Farber Cancer Institute, Wyss Institute, and the Department of Biochemistry and Molecular Pharmacology, Harvard Medical School, Boston Massachusetts, 02115, USA. [6]These authors contributed equally to this work. Correspondence should be addressed to S.R.P. (reck-peterson@hms.harvard.edu).

Nature Structural & Molecular Biology: doi:10.1038/nsmb.2205

Supplementary Figures

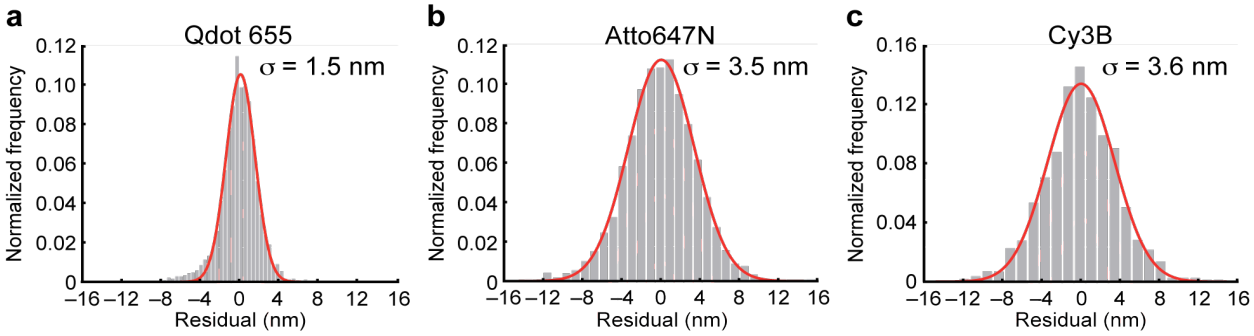

Supplementary Figure 1 Single-molecule localization precision. (**a–c**) To determine the precision of our single molecule measurements, we immobilized fluorophores separately on a coverslip and used a piezo nanostage to drive a staircase pattern of precise increments (6 nm for Qdot 655, 16 nm for both Atto647N and Cy3B). After each increment, at least 10 images were taken using the same exposure time and laser power as the experimental conditions used for tracking dynein. The point-spread function of individual fluorophores was fit with a 2-D Gaussian to determine their centroid position and a step-finding program was used to determine the average position after each increment. Histograms show the distribution of the difference between the raw centroid positions and the average positions between stage movements along one axis. The sigma value (the s.d. of the Gaussian fit) reports the localization precision of each fluorophore. (**a**) Qdot 655 (σ = 1.5 nm, N = 4041), (**b**) Atto647N (σ = 3.5 nm, N = 2378), (**c**) Cy3B (σ = 3.6 nm, N = 1632).

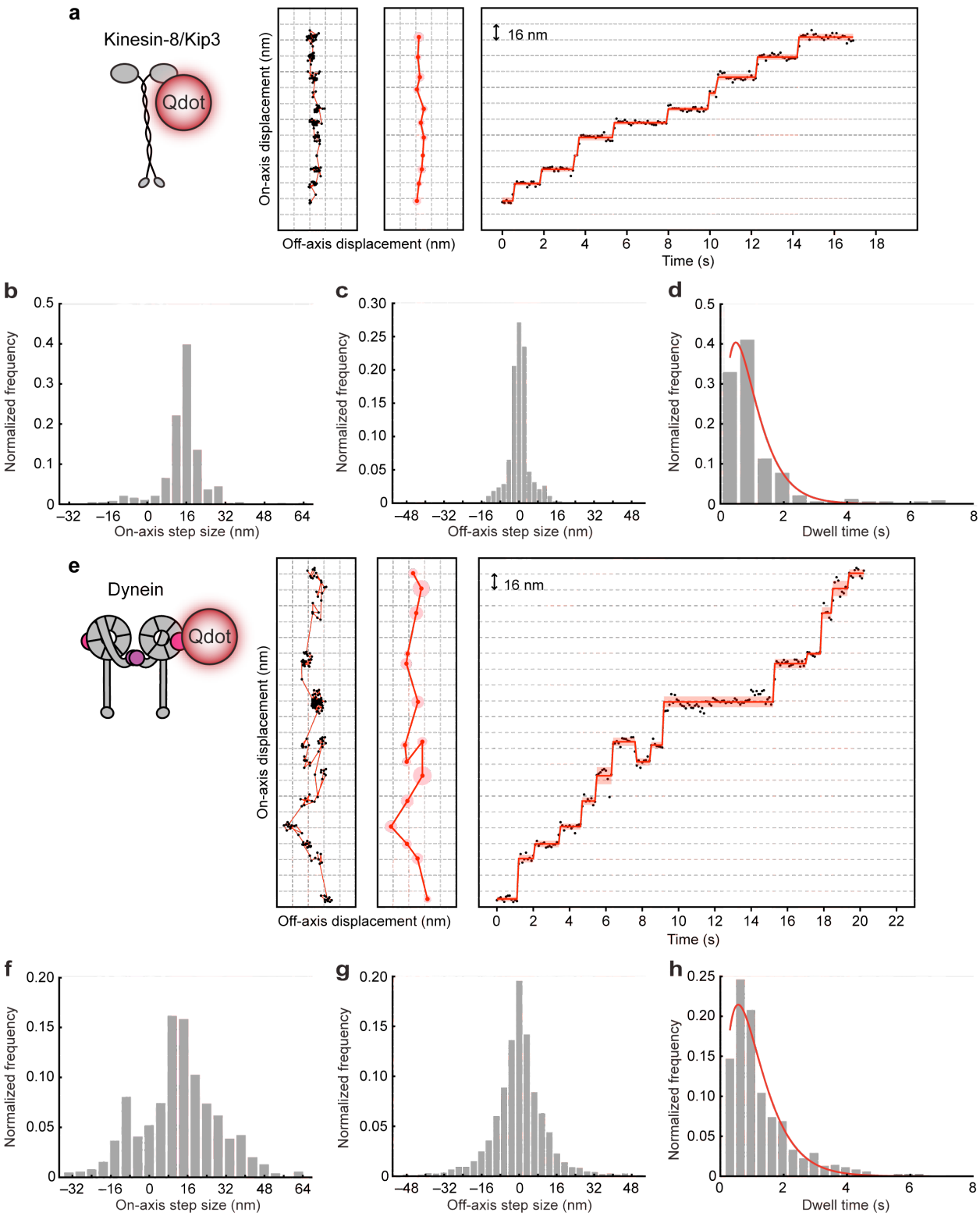

Nature Structural & Molecular Biology: doi:10.1038/nsmb.2205

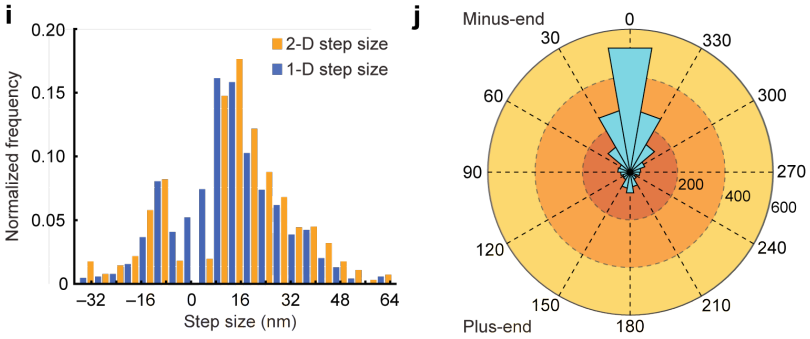

Supplementary Figure 2 Stepping behavior of motor domain labeled kinesin-8/Kip3 and dynein. (**a**) Representative one-color trace of kinesin-8/Kip3 labeled with a Qdot 655 attached to a single motor domain via a N- terminal HaloTag. Panel 1 shows the raw 2-D stepping data (black dots linked with red lines). Panel 2 shows the step positions as determined by a 2-D step finding algorithm (dark red circles and lines; lighter colored red circles represent the s.d.). All grid lines have 16 nm spacing. Panel 3 shows the 1-D on-axis projection of the 2-D steps. Black dots are the raw data, red lines are the steps determined by the 2-D step finding algorithm, and the light red bars indicate the s.d. of individual steps along the projection axis. (**b**) Histogram of the on-axis step size for motor domain labeled kinesin-8/Kip3. *N* = 384 for panels b–d. (**c**) Histogram of the off-axis step size for motor domain labeled kinesin-8/Kip3. 22%, 16%, and 11% of steps are greater than 4, 6 and, 8nm, respectively. (**d**) Histogram of dwell times for motor domain labeled kinesin-8/Kip3 fit to a convolution of two exponential functions with equal decay constants, with a rate of k = 2.06 $\pm$ 0.31 s^{-1}. Stepping data was acquired at 500 μM ATP every 100 ms. (**e**) Representative one-color traces of GST–dynein homodimers labeled with a Qdot 655 attached to a single motor domain via a C-terminal HaloTag. Panel 1 shows the raw 2-D stepping data (black dots linked with red lines). Panel 2 shows the step positions as determined by a 2-D step finding algorithm (dark red circles and lines; lighter colored red circles represent the s.d.). All grid lines have 16 nm spacing. Panel 3 shows the 1-D on-axis projection of the 2-D steps. Black dots are the raw data, red lines are the steps determined by the 2-D step finding algorithm, and the light red bars indicate the s.d. of individual steps along the projection axis. (**f**) Histogram of the on-axis step size for motor domain labeled GST–dynein. *N* = 1939 for panels f-h. (**g**) Histogram of the off-axis step size for motor domain labeled GST-dynein. 59%, 45%, and 36% of steps are greater than 4, 6, and 8 nm, respectively. (**h**) Histogram of dwell times for motor domain labeled GST-dynein fit to a convolution of two exponential functions with equal decay constants, with a rate of k = 1.78 $\pm$ 0.13 s^{-1}. Stepping data was acquired at 4 μM ATP every 100 ms. (**i**) Histograms of the 1-D and 2-D step sizes for motor domain-labeled dynein. The 2-D step size histogram reveals a peak at ~14–16 nm, while the 1-D step size histogram has a peak that is slightly smaller. 78% of the steps are forward steps. *N* = 2391 steps. (**j**) An angle histogram of the step angles. The step angle is defined as the angle between the step vector and the direction of on-axis movement. Steps to the left or right of the direction of motion are between 0° and 180°, or 180° and 360°, respectively. Steps between 90° and 270° are backwards steps. *N* = 2391 steps.

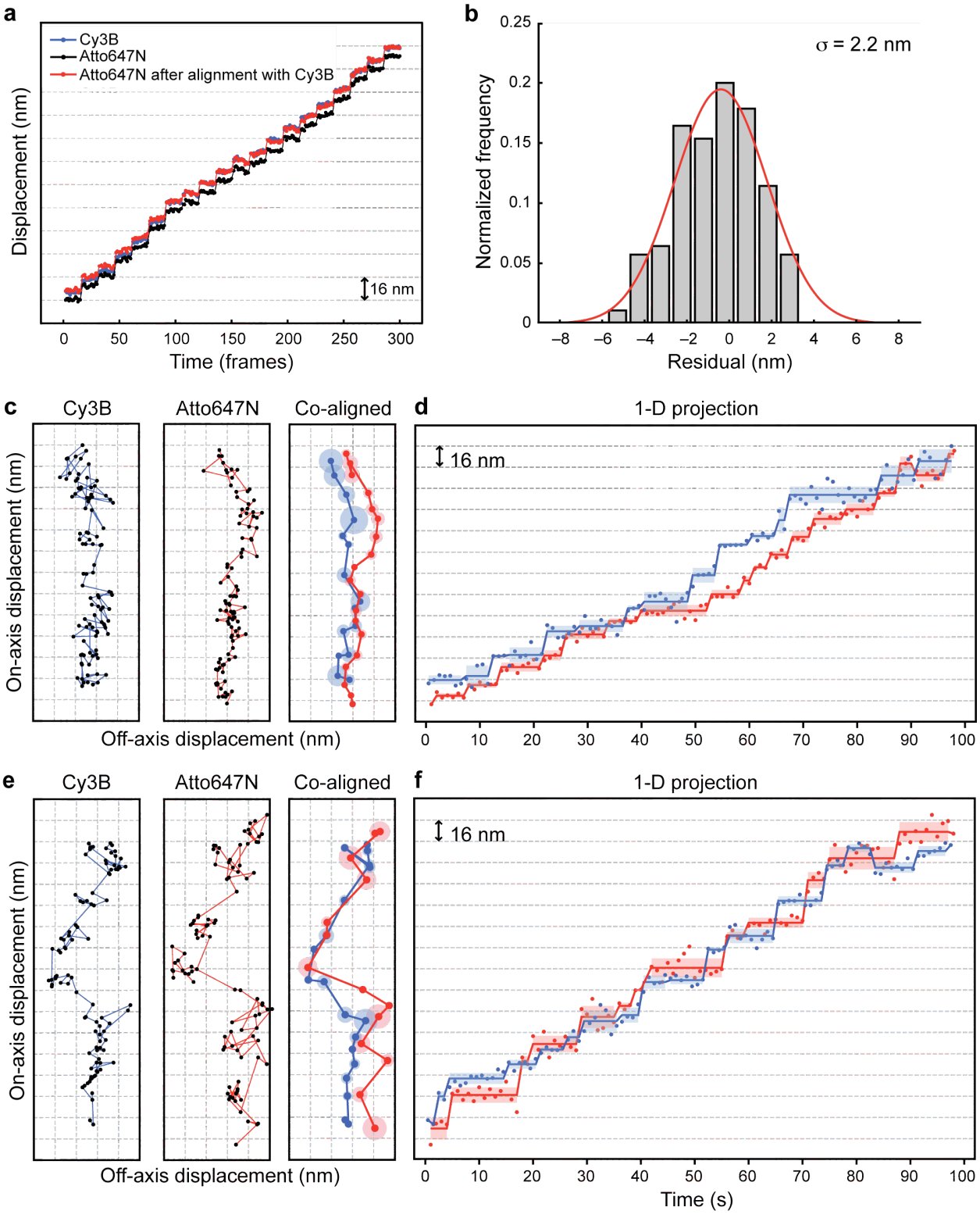
a
Cy3B
Atto647N
Atto647N after alignment with Cy3B
Displacement (nm)
16 nm
Time (frames)
b
σ = 2.2 nm
Normalized frequency
Residual (nm)
c
Cy3B
Atto647N
Co-aligned
On-axis displacement (nm)
Off-axis displacement (nm)
d
1-D projection
16 nm
e
Cy3B
Atto647N
Co-aligned
On-axis displacement (nm)
Off-axis displacement (nm)
f
1-D projection
16 nm
Time (s)

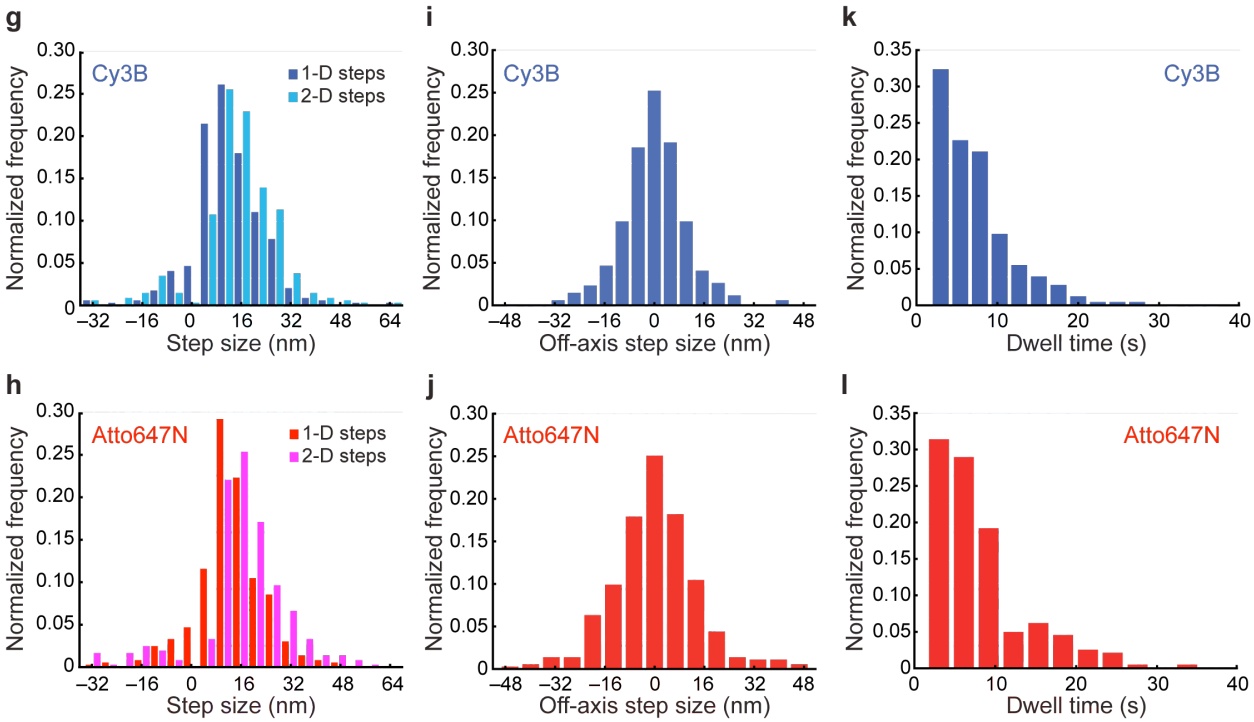

Supplementary Figure 3 Two color, high-precision, single molecule co-localization of dual labeled dynein heterodimers. (**a**) Validation of the single-molecule, high-resolution, co-localization method. Three stepping traces of a tetraspeck bead (Invitrogen, 0.2 mm) attached to the coverslip and driven in a 8 nm staircase pattern via a piezo nanostage (MadCity Labs) are shown. Cy3B channel (blue) and the Atto647N channel before alignment (black) and after alignment (red). (**b**) Histogram of the mapping accuracy for the alignment in (a). The mapping error for this alignment is ~2 nm as estimated by the s.d. of the difference between the stepping traces from Cy3B and Atto647N after alignment using a 2 μm X 2 μm alignment grid (see **Supplementary Methods**). (**c–f**) High-precision, two-color tracking of dynein stepping. (**c,e**) Representative two-color stepping traces of a DNA–dynein heterodimer. The raw 2-D positions (black dots in left and center panels) from a DNA–dynein heterodimer labeled with Cy3B (left panel, blue line) and Atto647N (center panel, red line). Co-alignment of the motor domain traces from each channel is shown in the right panel, with darker solid blue (Cy3B) and red (Atto647N) dots representing steps determined by a 2-D step finding algorithm, and larger, lighter-colored blue and red circles representing the s.d. of individual steps. (**d,f**) 1-D on-axis projection of the 2-D data from (c and e), with lighter blue and red bars representing the s.d. of individual steps along the projection axis. (**g-l**) Stepping statistics of the Cy3B- and Atto647N-labeled heads from the two-color experiments. 27 traces were analyzed for both channels. (**g,h**) Histograms of 1-D and 2- step size distributions. N = 345 steps (Cy3B); N = 363 steps (Atto647N). (**i,j**) Histograms of off-axis step size. N = 213 (Cy3B); N = 254 (Atto647N). (**k,l**) Histograms of dwell time distribution. Both distributions lacked a strong resemblance to a convolution of two exponential functions, possibly due to the fact that dynein's two motor domains do not always step alternately and/or because short dwells were under-sampled due to the time resolution of our method. N = 257 (Cy3B); N = 247 (Atto647N).

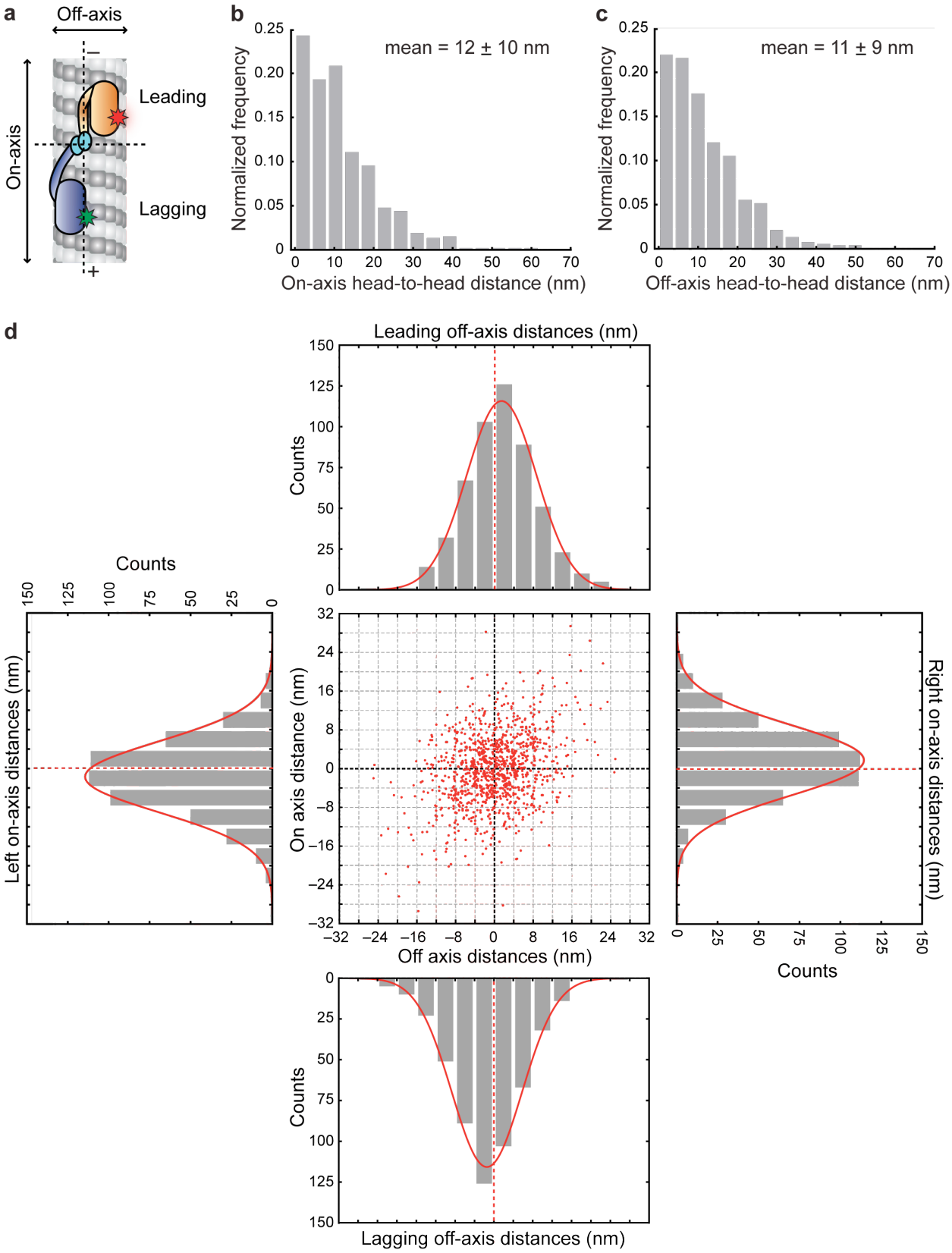
a
Off-axis
On-axis
Leading
Lagging
b
mean = 12 ± 10 nm
Normalized frequency
On-axis head-to-head distance (nm)
c
mean = 11 ± 9 nm
Normalized frequency
Off-axis head-to-head distance (nm)
d
Leading off-axis distances (nm)
Counts
Left on-axis distances (nm)
On axis distance (nm)
Off axis distances (nm)
Right on-axis distances (nm)
Lagging off-axis distances (nm)

Supplementary Figure 4 Distance between motor domains in the on- and off-axis directions. (**a**) Schematic showing leading and lagging head positions and the on- and off-axis microtubule directions. (**b**) Histogram of the on-axis component of the head-to-head distance. N = 523. (**c**) Histogram of the off-axis component of the head-to-head distance. N = 523. (**d**) A scatter plot of the relative positions of dynein's two motor domains during the two-head-bound state. This plot is similar to Figure 5c, however here all data (N = 523 dimers vs. 256 dimers in Figure 5c), including data that did not pass the t-test for left /right or leading/ lagging position determination, are included. As in Figure 5c, the centroid position of each motor is fixed at the origin. Each head position is then plotted (red dot) relative to this centroid. The leading and lagging head off-axis positions are shown in the histograms above and below the scatter plot. These off-axis distributions are significantly different from one another (one-tailed t-test, alpha level of 0.05, P = 6.7e–11). The distributions of left and right on-axis locations for all data points are shown in the histograms to the left or right of the scatter plot, respectively. The positions of the right and left head are significantly different from one another (one-tailed t-test, alpha level of 0.05, P = 4.3e–14). Gaussian fits of the histograms are shown in red.

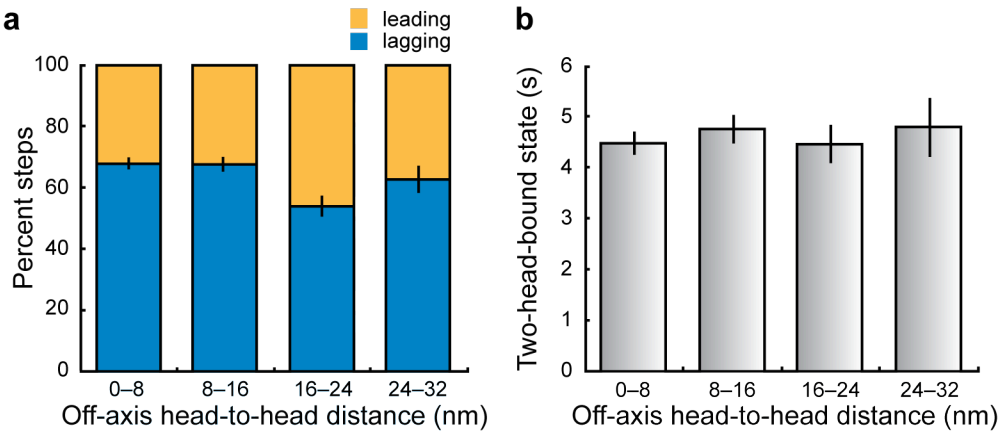

Supplementary Figure 5 Effects of tension are not observed in the off-axis direction. (**a**) Relative stepping probability of the leading and lagging heads as a function of the off-axis head-to-head distance. Error bars represent the s.e.m. generated by bootstrapping each bin 200 times. No trend between head-to-head distance and the probability of a leading or lagging head stepping was observed. *N* = 523. (**b**) The duration of the two-head-bound state as a function of the off-axis head-to-head distance. Mean durations are plotted with the error bars representing the s.e.m. There is no statistically significant trend between the duration of the two-head-bound state and the off-axis head-to-head distance (two-tailed KS-test, alpha level 0.05). *N* = 523.

Supplementary Tables

Supplementary Table 1 Yeast strains used in this study

Yeast Strain ID	Genotype	Source
VY208	MATa *his3-11,5 ura3-52 leu2-3,112 ade2-1 trp-1 pep4::HIS3 prb1Δ pGAL*-ZZ-TEV-EGFP-3XHA-GST-*dyn1*$_{331kDa}$-Gly-Ser-DHA[a]-KanR	[1]
VY268	MATa *his3-11,5 ura3-52 leu2-3,112 ade2-1 trp-1 pep4::HIS3 prb1Δ PAC11*-13Myc::*TRP pGAL*-ZZ-TEV-DHA-*dyn1*$_{331kDa}$	[1]
RPY897	MATa *his3-11,5 ura3-52 leu2-3,112 ade2-1 trp-1 pep4::HIS3 prb1Δ pGAL*-ZZ-TEV-EGFP-3XHA-SNAP[b]-Gly-Ser-*dyn1*$_{331kDa}$-Gly-Ser-DHA-KanR	This study
RPY1132	MATa *his3-11,5 ura3-52 leu2-3,112 ade2-1 trp-1 pep4::HIS3 prb1Δ pGAL*-ZZ-TEV-EGFP-3XHA-SNAPf[b]-Gly-Ser-*dyn1*$_{331kDa}$-gs-DHA-KanR	This study
PY6431	MATa *pGAL1*-6His-HALO-*KIP3*-LEU2(2μ) *prb1-122 pep4-3 reg1-501 gal1 ura3-52*	[2]

[a]DHA is the gene encoding the HaloTag (Promega). [b]SNAP and SNAPf are the genes encoding the SNAP-Tag (New England Biolabs).

Supplementary Table 2 Dimeric dynein motors used in this study

Yeast strain and oligo	Labels	Experiment
VY208	Halo–TMR	Run length and velocity assays, one-color high precision stepping assays
RPY897-Oligo A-NH2 & RPY897-Oligo A*-NH2	Halo–Atto647N Halo–TMR	Run length and velocity assays
VY268	Halo–biotin	One-color high precision stepping assays
RPY897-Oligo A-NH2-biotin & RPY897-Oligo A*-NH2	Biotin (on oligo)	One-color high precision stepping assays
RPY1132-Oligo A-NH2 & RPY1132- Oligo A*-NH2	Halo–Atto647N Halo–Cy3B	Two-color high precision stepping assays

Supplementary Methods

Protein purification and labeling

Dynein motors were purified as described previously[1] with the following modifications. Labeling reactions were performed during the purification, when the motors were bound via the N-terminal ZZ-tag to IgG sepharose beads (GE Lifesciences). GST-based dynein dimers were labeled with either 1 mM HaloTag–TMR (Promega) or 1 mM HaloTag–biotin (Promega) in TEV cleavage buffer (10 mM Tris (pH 8.0), 150 mM KCl, 10% (v/v) Glycerol, 1 mM DTT, 0.1 mM Mg-ATP and 0.5 mM PMSF) for 10 min at room temperature. Dynein monomers for subsequent dimerization with DNA were labeled with 20 μM BG-oligo with or without 2 μM HaloTag–fluorophore in TEV cleavage buffer for 30 min at room temperature. After dynein labeling, the beads were washed an additional 4 times with TEV cleavage buffer to remove unbound BG–oligos and HaloTag–fluorophores. The purification was then completed as previously described[1].

The oligomer sequences used for labeling were as follows: Oligo A-NH2 (Amine - GGT AGA GTG GTA AGT AGT GAA), Oligo A*-NH2 (TTC ACT ACT TAC CAC TCT ACC – Amine), Oligo A-NH2-biotin (Amine - GGT AGA GTG GTA AGT AGT GAA - Biotin), Oligo A* (TTC ACT ACT TAC CAC TCT ACC). The pairs of dynein protomers used for different experiments are listed in **Supplementary Table 2**.

Formation of dynein heterodimers was detected using a PAGE gel shift assay that did not denature the duplex DNA. Dynein solutions with complimentary oligos were mixed and incubated on ice for 15 min and then mixed with LDS sample buffer (Invitrogen) and separated on 3–8% tris-acetate gels (Invitrogen). Dynein was visualized with SYPRO red protein stain (Sigma), GFP fluorescence (present on the tail domain of VY208, RPY897, and RPY1132), or the covalently linked HaloTag–fluorophores. Typically, 65% (SNAP-tag) or 90% (SNAPf-tag) of the dynein protomers formed heterodimers. The only difference between these tags is the kinetics of the SNAP-tag ligation to its BG substrate. The much higher heterodimer formation achieved with the SNAPf-tag allows us to conclude that the yield of DNA-based dimerization is limited by the efficiency of linking SNAP-tagged monomers to BG–oligos, not by the efficiency of DNA hybridization. To minimize protein degradation, we chose to use short labeling times that resulted in incomplete oligo labeling of SNAP-tagged dynein monomers.

For the run length and velocity assays, inactive motors that could bind microtubules, but not release, were removed by a microtubule affinity step in the presence of MgATP. Dynein was mixed with 0.1 volumes of 60 μM taxol-stabilized microtubules and 0.2 volumes 5X TEV cleavage buffer supplemented with 50 μM taxol and incubated at room temperature for 10 min. The mixture was centrifuged at 108,000 x g for 15 min at room temperature. The dynein-containing supernatant was aliquoted, snap frozen in liquid nitrogen, and stored at –80°C.

Microtubules were purified from bovine brain and axonemes from sea urchins[4]. In order to compare our current results with previously published work[1], we used axonemes for the experiments shown in Fig. 2, Supplementary Fig. 2, and Fig. 3. All other experiments used bovine brain microtubules.

Single molecule run length and velocity assays

Flow chambers were made by attaching a coverslip to a glass slide with double-sided tape. The flow chamber was then incubated with one chamber volume (~10 μl) of 1mg/ml biotin–BSA in BRB80 (80 mM PIPES (pH 6.8), 2 mM $MgCl_2$, and 1 mM EGTA) for 2 min at room temperature. Unbound free biotin–BSA was removed by washing the chamber with 4 chamber volumes of BRB80. The chamber was next perfused with 20 μl of 0.5 mg/ml streptavidin in BRB80 and incubated at room temperature for 2 min, washed with 4 chamber volumes of dynein lysis buffer (1X dynein lysis buffer: 30 mM HEPES (pH 7.2), 50 mM KAcetate, 2 mM MgAcetate, 1 mM EGTA, 10% (v/v) glycerol, 1 mM DTT, 0.1 mM Mg-ATP and 0.5 mM PMSF) supplemented with 20 μM taxol, but lacking ATP and PMSF, to remove excessive unbound streptavidin, and incubated with 10 μl taxol-stablized bovine microtubules (containing 10% Hilyte Fluor 488 (Cytoskeleton Inc.) labeled tubulin and 10% biotinylated tubulin (Cytoskeleton Inc.)) at room temperature for 2 min. Finally, the chamber was perfused with dynein motors diluted in dynein motility buffer (30 mM HEPES (pH 7.2), 50 mM KAcetate, 2 mM MgAcetate, 1 mM EGTA, 10% (v/v) glycerol, 1 mM DTT, 1 mM MgATP, 1.25 mg/ml casein and 20 μM taxol) and supplemented with an oxygen scavenger system as previously described[1]. The sample was alternately excited with the 561 nm and 640 nm lasers. Interspersed time-lapse image sequences were acquired at 1 frame per 2 s with an exposure time of 100 ms (typically for 10 min). Kymographs were generated and analyzed in ImageJ (NIH). Only those runs that were visible in both color channels were scored to ensure that all data came from dual labeled dynein heterodimers.

Calibration of the TIRF microscope for high precision experiments

Three different fluorophores (Qdot 655, Cy3B and Atto647N) were used for high-precision measurements in this study. For each fluorophore, we determined the localization precision achievable under typical experimental conditions. We first immobilized the fluorophore on a coverslip, and moved the coverslip in a staircase pattern of precise increments (6 nm for Qdot 655 and 16 nm for both Cy3B and Atto647N) using a piezo nanostage (MadCity Labs). Between stage movements, multiple images were taken using laser powers and exposure times identical to experimental conditions. The point-spread function of individual fluorophores were then fit with a 2-D Gaussian to determine their centroid position[3], and the average positions of the fluorophores between stage movements were determined by a custom MATLAB (The MathWorks) program (see below). To estimate the localization precision, we next computed the difference between the raw centroid positions and the average positions from the step-finding program (**Supplementary Fig. 1a–c**).

One-color high precision motility assays

All one-color high precision motility assays were performed with dynein singly-labeled via a N- or C-terminal HaloTag with a Qdot 655 (Invitrogen) on sea urchin axonemes[4] at room temperature. Previously, we

observed that the large (15–20 nm) diameter of Invitrogen's Qdot 655 allowed labeling of only one motor domain within dimeric GST–dynein (even though both motors contained a labeling site), suggesting one site is sterically blocked[1]. The flow chamber was first incubated with one chamber volume of axonemes in BRB12 (12 mM PIPES (pH 6.8), 2 mM $MgCl_2$ and 1 mM EGTA) for 2 min to allow axonemes to adhere to the coverslip, and was washed with 10 chamber volumes of BRB12 to remove unbound axonemes. The chamber was then washed with dynein lysis buffer, incubated with 10 μl of biotinylated dynein molecules in the absence of ATP for 2 min, washed with 10 chamber volumes of dynein motility buffer to remove unbound dynein molecules, and incubated with 50 nM Qdot 655 streptavidin (Invitrogen). The labeling reaction was performed with dynein sparsely immobilized on axonemes to prevent biotinylated dynein molecules from aggregating on the streptavidin coated Qdots. High precision stepping experiments were performed in dynein motility buffer with 10 mM β-mercaptoethanol (in place of DTT) and 4-6 μM Mg-ATP (in place of 1mM ATP), supplemented with an ATP regeneration system (10 mg/ml pyruvate kinase and 10 mM phosphenolpyruvate) and an oxygen scavenger system[1]. The sample was excited with the 405 nm laser at ~5 mW. Time-lapse image sequences were stream acquired with 100 ms exposure time for 40–50 s. Fluorescent spots in the original images were then fit with a 2-D Gaussian to precisely localize their position[3]. Steps (1-D and 2-D) were determined by a custom MATLAB program (see below).

Two-color high precision motility assays

For all two-color high precision experiments, we used DNA-based dynein heterodimers formed from two complimentary DNA-linked dynein protomers labeled with HaloTag–Cy3B and HaloTag–Atto647N at the C terminus. Sample slides were prepared as described above for the two-color run length and velocity assays with the following modifications: (1) Stepping experiments were performed using unlabeled (instead of fluorescent) taxol-stabilized microtubules to minimize crosstalk between fluorophores. (2) The chambers were incubated with dynein motors in the absence of ATP for 2 min before an extensive wash with 5 chamber volumes of motility buffer lacking ATP to remove unbound dynein molecules. (3) Stepping experiments were performed in a dynein motility buffer lacking 50 mM KAcetate, supplemented with 500 nM ATP (instead of 1 mM ATP) and 2 mM Trolox (which improved the photostability of both Cy3B and Atto647N; instead of 10 mM β-mercaptoethanol). The sample was alternately excited with the 561 nm and 640 nm lasers (the power for each was ~10 mW at the objective), and interspersed time-lapse image sequences were stream acquired at an exposure time of 600 ms for a total duration of 2–3 min.

A custom MATLAB program was used to screen for dual-labeled dynein molecules from the raw two-color image sequences. Dual-labeled dynein molecules were tracked with a 2-D Gaussian function to precisely localize their centroid locations in both the Cy3B and Atto647N channels throughout the image sequence. The resulting stepping traces (x-y coordinates of dynein's centroid positions) and the corresponding fluorescence intensity profiles were then plotted independently for the Cy3B and Atto647channels. At this point the data from each channel was visually inspected and traces were discarded for the following reasons: (a) if the stepping dwell clusters were not clearly defined; (b) if the fluorescence intensity was too low to yield high

precision localization; (c) if the observable step sizes were much larger than the known dynein step size distribution (indicating missed steps); or (d) if multiple-step photobleaching was observed based on the fluorescence intensity profile (indicating the presence of more than 1 dye per dynein head).

Two color stepping traces that passed the screening process were next precisely co-localized using an alignment procedure described previously[5]. Briefly, we created an alignment grid surrounding each candidate two-color trace pair by immobilizing a 0.2 mm tetraspeck bead (Invitrogen) on a coverslip and moving it in a grid pattern (2.2 μm X 2.2 μm with a spacing of 200 nm) with a piezo nanostage (Madcity Labs). Fiducial data was acquired in both imaging channels at each grid point. This mapping method yielded a mean accuracy of ~4 nm as determined by the target registration error[5]. We validated the alignment method by precisely aligning the positions of a tetraspeck bead determined from the two imaging channels (**Supplementary Fig. 1d,e**). Aligned candidate two-color traces were next analyzed using a custom MATLAB 2-D stepping program (see below) to determine steps in 1-D and 2-D. Steps were discarded at this stage if a stretch (more than three) of dwell-clusters could not be identified in both channels. The remaining two-color stepping traces were further processed with the temporal and spatial analysis. Our dwell and step analyses only included trace regions where we could confidently define the spatial and temporal relationships between the Cy3B and Atto647N channels.

Two-dimensional step finding algorithm

To determine dynein's step size and dwell time (the length of pausing between steps), we used an extended Chung-Kennedy edge-detecting algorithm[6] specifically designed for analyzing noisy time series[7]. This algorithm uses running averages in the forward and backward directions, as well as the estimated noise of the trace, to calculate a probability function for the presence or absence of steps at a given point in time. A threshold is then suggested for statistically assigning steps. We implemented this filter in an automated step-detecting program in MATLAB, with parameters suggested by Smith et al[7]. In order to detect steps, a stepping trace (or a two-color stepping trace pair) was first analyzed using principal component analysis and the direction of longer variance of the trace, which corresponds to the principal axis of motion, was aligned to the X-axis. Subsequently, the edge detector algorithm was independently applied to the x (on-axis) and y (off-axis) components of the trace to find a stepping pattern in each direction. Steps were called when they had a component of either $\geq$ 4 nm on-axis (half the size of a tubulin dimer), $\geq$ 5 nm off-axis (the separation between two adjacent tubulin protofilaments), or both.

The suitability of this step-finding method was assessed by comparing the stepping statistics of Cy3B- and Atto647N- labeled dynein heads with that of the less noisy Qdot-655 labeled dynein head. Even with the lower precision of the organic fluorophore data, both the on- and off-axis step size distributions of the Cy3B- and Atto647- labeled heads (**Supplementary Fig. 3g–j)** were similar to the stepping statistics of the much brighter Qdot-655 labeled dynein head (**Supplementary Fig. 2f,g**), suggesting that our step assignments for the two-color data are accurate.

Stepping and dwell analysis

A custom MATLAB program was used to analyze the data of fitted x and y positions determined by the step finding program. The program used the following criteria to perform independent spatial and temporal analyses on the steps and allow for correlation analysis. For the heads to be called as leading, lagging, or uncertain, the on-axis positions of the two heads are compared using a two-sample t-test with a confidence level of 95%. The same spatial analysis was applied to the off-axis direction to call heads left, right, or uncertain. A passing step was defined as a switch in on-axis position (e.g. a leading head became a lagging head) while a not-passing step maintained the relative on-axis position of the two heads. If the relative position of the heads before or after a step was uncertain, the step was not called as passing or not passing. The same analysis was applied in the off-axis direction to determine whether the heads crossed from left to right.

For steps to be analyzed as alternating or not alternating, they had to be clearly resolvable in the time domain. Sequential steps were considered for this analysis only if both the step in question and the previous step were sufficiently resolvable in time. We defined a step as resolvable in time if it was at least one frame away from a step in the other channel. The head-to-head distance was calculated for all positions where the heads remained stationary for at least 3 points of overlap (two points in one channel and one point in the other). This was calculated in both the x and y directions as the difference between the Cy3B and Atto647N positions.

The 2-D head-to-head distance and step size were calculated by measuring the magnitude of the vector composed of the on- and off-axis components.

Histograms

For all histograms with 1 variable, the bin width was determined using Scott's rule[8]. For all histograms with 2 variables, the bin width was determined using Scott's rule on the first variable. For ease of visually comparing the two variables, the width of each variable's bar is 40% of the total bin width and the first variable is plotted in a position that is located at the bin center –0.25*bin width, while the second variable is plotted in a position that is located at the bin center +0.25*bin width.

Supplementary References

1. Reck-Peterson, S.L.*, et al.* Single-molecule analysis of dynein processivity and stepping behavior. *Cell* **126**, 335–348 (2006).
2. Su, X.*, et al.* Mechanisms underlying the dual-mode regulation of microtubule dynamics by Kip3/kinesin8. *Mol Cell* **43**, 751–763 (2011).
3. Thompson, R.E., Larson, D.R. & Webb, W.W. Precise nanometer localization analysis for individual fluorescent probes. *Biophys J* **82**, 2775–2783 (2002).
4. Waterman-Storer, C.M. Microtubule organelle motility assays. in *Current Protocols in Cell Biology* (eds. Bonifacino, J.S., Dasso, M., Harford, J.B., Lippincott-Schwartz, J. & Yamada, K.M.) (John Wiley, NY, NY, 2001).
5. Churchman, L.S., Okten, Z., Rock, R.S., Dawson, J.F. & Spudich, J.A. Single molecule high-resolution colocalization of Cy3 and Cy5 attached to macromolecules measures intramolecular distances through time. *Proc Natl Acad Sci U S A* **102**, 1419–1423 (2005).
6. Chung, S.H. & Kennedy, R.A. Forward-backward non-linear filtering technique for extracting small biological signals from noise. *J Neurosci Methods* **40**, 71–86 (1991).
7. Smith, D.A. A quantitative method for the detection of edges in noisy time-series. *Philos Trans R Soc Lond B Biol Sci* **353**, 1969–1981 (1998).
8. Scott, D.W. On optimal and data-based histograms. *Biometrika* **66**, 605–610 (1979).